J. COMBIN. MATH. COMBIN. COMPUT. 127a (2025) 5945--5966

Journal of Combinatorial Mathematics and Combinatorial Computing
www.combinatorialpress.com/jcmcc

Combinatorial Press

# Research on the picture hierarchy enhancement technique based on probability distribution in oil paintings

Baoqun Wang[1, ✉]

[1] *School of Fine Arts and Design, Huainan Normal University, Huainan, Anhui, 232038, China*

ABSTRACT

With the rapid development of computer vision technology, image enhancement technology involves an increasingly wide range of research content. At the current stage, picture hierarchy enhancement technology is a research hotspot in the field of image enhancement. This paper proposes an oil painting image enhancement network based on positive probability distribution guidance. The multidimensional spatial information of the samples is obtained through the multibranch information extraction architecture in the network structure, and the probability distribution estimation module estimates the probability distribution through the obtained multidimensional spatial information. In addition, a new image enhancement method based on the RGB color balance method is proposed, which combines the multi-scale Retinex enhancement algorithm with color recovery and the RGB, Lab color space histogram adaptive stretching algorithm, to further improve the effect of oil painting image display. The experimental results show that the method has a better image color bias correction effect compared with the existing techniques. In terms of subjective evaluation, the average subjective score of this paper's method in three different aesthetic levels reaches 9.15, obtaining a high evaluation. The samples enhanced based on this paper's algorithm all obtained high aesthetic index scores, indicating that the oil paintings under this paper's algorithm are in line with the public aesthetics, which is of great significance to the work of oil painting artists.

*Keywords:* Positive probability distribution, Image enhancement, Color balance, Color correction, Lab color space

## 1. Introduction

Layering in painting refers to the feeling of the depth of the picture, which gives the picture a sense of three-dimensionality and space. Layering is a very important aspect in painting because it can make the picture more vivid and real [1]. In painting, perspective is the most basic technique, which can determine the depth and spatial sense of the picture, and through perspective can add a sense of depth to the picture and make the distance and proximity of the picture more obvious [2]. Color contrast or

✉ Corresponding author.
*E-mail address:* Wbqun2012@hnnu.edu.cn (B. Wang).
Received 15 January 2024; Revised 10 March 2024; Accepted 30 November 2024; Published Online 15 April 2025.
DOI: 10.61091/jcmcc127a-328

layering can also enhance the sense of hierarchy in the picture and make the picture richer, such as when using red and green, the red will be more prominent in the picture, which is the effect of color contrast [3-4]. In addition, there is a contrast between light and dark by adding shadows and highlights, as well as the processing of details can make the picture more vivid and real.

Oil painting is an art form that expresses emotions through visual elements such as color, line and shape. Oil paintings have multi-level artistic appeal, namely, color level, texture level, hierarchy level, and fluidity level [5]. Among them, the expression of layering is one of the unique charms in oil paintings. Through the overlapping of pigments and soft transition, oil paintings can show a variety of layered sense. For example, in a landscape painting, the oil painter can use the technique of transparent layers to express the relationship between the mountains and the water by using different concentrations and shades of color, making the picture more three-dimensional and spatial sense.

A probability distribution is a statistical tool used to measure the likelihood of each outcome of a random event. In statistics, probability distribution is often used to describe continuous random variables and discrete random variables [6]. Continuous random variables refer to variables that may take on any real value, such as height, weight, etc., while discrete random variables refer to variables that can only take on a series of discrete values, such as the heads and tails obtained by flipping a coin, the number of points in a die, etc. [7-8]. Since the oil painting picture hierarchy is more of an opposing expression of color, light and dark and personal feeling, how to enhance the picture hierarchy under random conditions outside the work through other methods on the basis of the work's immutability is a topic of research value. For this reason, this paper uses the probability distribution to explore.

The article combines the image enhancement architecture based on positive probability distribution guidance and the RGB-based color balance method to accomplish the task of picture hierarchy enhancement of oil paintings from two aspects: oil painting quality enhancement and oil painting color and brightness enhancement. Multi-branch information extraction architecture combining spatial attention, pixel attention and channel attention branches is designed for multi-dimensional spatial features of mixed samples. Preliminary color correction of oil paintings is carried out by RGB color balance method, and MSRCR algorithm is applied to further enhance the color correction effect of oil paintings. The oil painting color is further enhanced by using relative global histogram stretching algorithm. The color and brightness of the image are adaptively stretched in Lab color space to obtain the final enhanced oil painting image. In this paper, experiments are designed to verify the image color bias correction and quality enhancement effect of this paper's algorithm, and the overlap between the oil paintings enhanced by this paper's algorithm and the popular aesthetics is verified in practical applications.

## 2. Overview

Most of the current research on oil paintings by scholars is at the level of protection, restoration, categorization, style transfer generation, and intelligent creation of oil paintings. For example, literature [9] introduces artificial intelligence combined with image analysis and environmental monitoring to provide protection and repair for oil paintings, as well as combining traditional techniques to clean and protect the picture of oil paintings. For protection, chemical methods can also be used, and literature [10] achieved multiple levels of protection by adding molybdenum trisulfide nanoparticles to oil paintings by reducing microbial damage, reducing dirt buildup, and resisting ultraviolet rays on oil painting canvases. Literature [11] visualized the brush strokes in oil paintings by machine learning algorithms supported by reflection transform imaging technology, and classified the oil paintings by this visualized information. Literature [12] modified the generative adversarial network using gradient penalty, combined with the constructed total variance loss function to study the style transfer and reconstruction of image oil paintings, after the transfer of the oil painting image with good edges and texture levels. Literature [13] used computer image processing technology to construct an oil painting creation model from the three aspects of digital painting, stroke direction, and color transformation, and obtained 65% and more favorable comments. And the sense of hierarchy as a major focus of oil painting appreciation, its performance not only makes the oil painting works more full and three-dimensional, but also provides a selective visual experience for the viewer.

## 3. Enhanced picture hierarchy based on probability distribution

### *3.1. Color space model*

The colors of nature as seen by humans are varied, and the colors seen by the human eye are determined by the visible light reflected from objects. The color image produced by a device or media may be different from what the human eye sees, and different devices have different color spaces to detect and display. Therefore, quantitative representation of color is an essential part of the process. As different fields have different requirements for color display. Researchers and scholars have accordingly proposed a variety of color space models to define colors based on these different requirements.

3.1.1. RGB color space. A large number of color optics experiments have shown that any color can be quantified and described by a combination of the three primary colors, red (R), green (G), and blue (B). Red, green and blue are called base colors because these three colors cannot be composed of any other color mixture, and these three colors are independent of each other. The three base colors are combined in different proportions. By combining them, it is possible to obtain different colors. This color space can be represented in the Miaokal three-dimensional cubic coordinate system, with the three base colors corresponding to the axes in the cubic coordinate system. All colors are in this space, for example black is located at the origin with coordinates (0,0,0) and white is located at the vertex furthest from the origin with coordinates (1,1,1). The coordinates of each color point in the color space are represented by coordinate values representing the red, green, and blue components. Obviously, the capacity of the color space is much larger than that of the grayscale space, which also proves from the fact that the grayscale image occupies less space.

3.1.2. Lab color space. Lab color space [14] is a color space designed and proposed by the International Commission on Illumination (CIE). Lab space is a kind of space describing color display, it is a kind of spatial model related to the visual characteristics of the human eye but not related to the display device. Lab color space is able to express more colors than the RGB space, which belongs to the inclusion relationship, and any color existing in the RGB space can be expressed in Lab space. Any color that exists in RGB space can be expressed in Lab space. If the Euclidean distance between two color points in Lab space is larger, then the visual effect difference between these two colors in human eyes will be larger.

The Lab color space schematic consists of three components: component $L$, which represents luminance, and components $a$ and $b$, which represent saturation. Component $L$ can represent the luminance of a color point from black to white. Chroma Component $a$ represents the color component of a color point from pure green to positive red. Chrominance component $b$ can represent the blue to yellow color component of a color point.

RGB space is usually converted to Lab space by using $XYZ$ color space as an intermediate. The steps to convert RGB space to $XYZ$ color space are as follows:

1) Normalize the $R$, $G$ and $B$ components of the image:

$$\begin{cases} R = R' / 255 \\ G = G' / 255 \\ B = B' / 255 \end{cases} \tag{1}$$

$P \in \{R', G', B'\}$ denotes the original component $P$ of the image in RGB space and $I \in \{R, G, B\}$ denotes the normalized component $I$ of the image.

2) Gamma transform the normalized components $R$, $G$, $B$ of the image:

$$I = \begin{cases} \left(\frac{I+0.055}{1.055}\right)^{2.4}, (I > 0.04056) \\ \frac{I}{12.92}, Other \end{cases} \left(I \in \{R, G, B\}\right) \tag{2}$$

3) The $R$, $G$, and $B$ components of the image are then linearly transformed into the $X$, $Y$, and $Z$ components:

$$\begin{bmatrix} X \\ Y \\ Z \end{bmatrix} = \begin{bmatrix} 0.4125 & 0.3576 & 0.1804 \\ 0.2127 & 0.7152 & 0.0722 \\ 0.0193 & 0.1192 & 0.9502 \end{bmatrix} \cdot \begin{bmatrix} R \\ G \\ B \end{bmatrix} \tag{3}$$

$Q \in \{X, Y, Z\}$ represents the $Q$ component of the image in $XYZ$ space.

The steps to transform $XYZ$-space to Lab-space are as follows:

(1) Perform a nonlinear transformation on the $X$, $Y$, and $Z$ components of the image:

$$Q = \begin{cases} Q^{1/3}, Q > \left(\frac{6}{29}\right)^3 \\ \left(\frac{1}{3}\right)\left(\frac{29}{6}\right)^2 \cdot Q + \frac{16}{116}, Other \end{cases} \left(Q \in \{X, Y, Z\}\right) \tag{4}$$

(2) The $X$, $Y$, and $Z$ components of the image are then linearly transformed into the $L$, $a$, and $b$ components:

$$\begin{cases} L = 116 \cdot Y - 16 \\ a = 500 \cdot (X - Y) \\ b = 200 \cdot (Y - Z) \end{cases} \tag{5}$$

$U \in \{L, a, b\}$ denotes that the image is $U$-component in Lab space.

3.1.3. HSI color space. HSI is a color space closely related to visual perception [15]. It is more consistent with the effect of color perception by the human eye than other color spaces. Components $H$, $S$, and $I$ represent hue, saturation, and luminance, respectively, where components $H$ and $S$ reflect the color information of the pixel, and component $I$ reflects the intensity of the pixel. The angle of the circular ring in the schematic diagram of the HSI space represents the hue of the color $H$, and different angles correspond to different colors, e.g., 0 degrees means red. The horizontal distance from the center of the ring to the color point represents the saturation $S$, different distances correspond to different saturation, for example, the saturation of the color point on the edge of the ring is 1, while the saturation of the color point inside is between 0 and 1. The brightness $I$ is represented by the vertical distance from the color point to the center of the ring, and the further the distance, the higher the brightness.

The conversion relationship between HSI space and RGB space is as follows:

$$\begin{cases} I = \frac{1}{3}(R+G+B) \\ S = 1 - \frac{3}{R+G+B}[\min(R,G,B)] \\ H = \arccos\left\{ \frac{[(R-G)+(R-B)]}{2\left[(R-G)^2+(R-B)(G-B)\right]^{1/2}} \right\} \end{cases} \tag{6}$$

$M \in \{H,S,I\}$ represents the $M$ component of the image in HSI space, which unlike RGB space, HSI color space separates the hue and luminance of a pixel point from each other. The $H$ and $S$ channel values, which are related only to the properties of color as perceived by the human eye, are independent of the brightness of the pixel. The $I$ -channel values are independent of the color of the pixel, only the luminance, and the principle of the HSI space coincides with the human eye's perceptual properties, which makes it more suitable for applications oriented towards human perception than the RGB space. When we need to change the color of a pixel (e.g. brightness) in HSI space, we only need to adjust its $I$ coordinates, not the values of the three components as in RGB space.

### *3.2. Hierarchical Enhancement of Oil Painting Texture Based on Positive Probability Distribution*

The algorithm proposed in this paper consists of two core components: a multi-branch information extraction architecture and a probability distribution estimation module (PDEM), in which the multi-branch information extraction architecture mainly utilizes pixel convolutional blocks, channel convolutional blocks, and spatial convolutional blocks to obtain the pixel, channel, and spatial information weights from the input features, and also introduces a dense convolutional block to obtain the deep semantic information. The probability distribution estimation module, on the other hand, obtains the probability distribution of a clear image from a mixture of samples by calculating the mean and variance of the feature image and guides the network to enhance the degraded image.

The structure is designed to extract the multidimensional spatial significance from the input features to provide sufficient feature information for the subsequent calculation of probability distributions, which in turn improves the enhancement capability of the network, and the internal structure is shown in Fig. 1.

In Figure 1: Conv2d denotes the convolution unit, $l \times l$ is the convolution kernel size, and $C$ is the number of output channels.

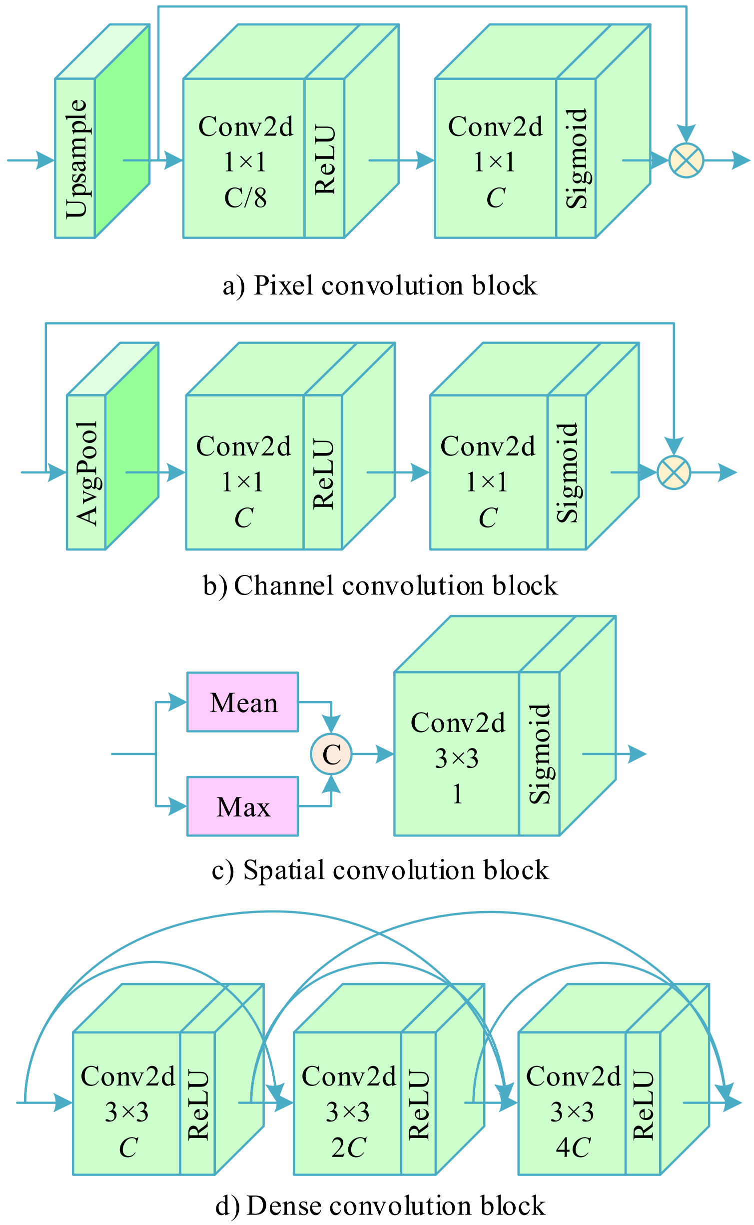


**Fig. 1.** The structure diagram of the internal module

Fig. 1a) shows the pixel convolution block structure, which first uses an upsampling operation between pixel points using bilinear interpolation to enlarge the length and width of the input feature image by a factor of two of the original, thus improving the utilization of the pixel information, and then a pixel-by-pixel process is performed on the feature image using a convolutional unit of size $1\times1$, and the output is obtained using the Sigmoid activation function, Eq:

$$V_{\text{Sigmoil}}(x)=\frac{1}{1+\mathrm{e}^{-x}} \tag{7}$$

In the attention mechanism [16], compared with the ReLU activation function, this function not only captures and smoothes out the subtle changes in the mapping output more accurately, but also suppresses the effects of mutated features more effectively during the subsequent operation with element multiplication. Finally, the computed pixel weights are incorporated into the input features by elemental multiplication.

Fig. 1b) shows the structure of the channel convolution block. Given the different attenuation levels of the three color channels in the oil painting image, the structure uses channel attention to extract the channel weight information of the input features. As shown in the figure, in order to ensure that the subsequent convolution units can capture the channel weights of the feature images more effectively, the image size is first reduced from $H \times W \times C$ to $1 \times 1 \times C$ using the global average pooling operation; then the $1 \times 1$-convolution unit is applied to extract the channel weights and output them through the Sigmoid activation function; finally, the channel weights are combined with the input features through the elemental multiplication operation, so that the channels get the corresponding weights assigned to them.

In order to maintain the integrity of the input image, this paper also introduces the spatial attention module to focus on the overall spatial information of the image, the structure is shown in Fig. 1c).

This module first averages and maximizes the dimensions of the input features, changing their size from $H \times W \times C$ to $H \times W \times 1$. Then the information is fused using the fully connected operation, and the pixel information of the image is further extracted by the $3 \times 3$ convolution unit. Finally, the Sigmoid activation function is used to enhance the network's ability to perceive details and globalities within the feature image space.

The information carrying capacity of the degraded image of the oil painting is directly related to the efficiency of the subsequent machine vision tasks. Therefore, in this paper, a dense connected module containing three layers of convolutional units is designed to extract the deep semantic information of the image, and the structure is shown in Fig. 1d). The module integrates the information extracted from the front layer of convolutional units into all the subsequent layers to improve the utilization of feature information while increasing the depth of the network, which makes the module focus on the extraction of deep semantic information.

In summary, the processing flow of the multi-branch information extraction architecture is as follows: first, mixed samples of clear and degraded images are input into the module during the training process. Second, the multidimensional spatial information is extracted from the mixed samples of clear and degraded images, and the spatial information is gradually added to the dense convolutional block through the fully connected operation. Finally, the spatial information is directly output to the next unit to prevent information loss during fusion.

3.2.1. Probability distribution estimation module. Most deep learning algorithms based on supervised learning use an end-to-end training model to improve the network performance, while ignoring the weight transformations in the middle part of the network, which usually leads to over-enhancement or under-fitting problems. To address this problem, this paper uses a probability distribution estimation module that estimates the probability of the enhancement distribution of a clear image from a mixture of samples, which guides the network to recover the degraded image.

The main purpose of this module is to extract the enhancement distribution that converts the degraded image into a clear image from the mixed samples. Therefore, firstly, the mean and variance matrices for each channel of the mixed samples and the degraded feature samples are computed with a size of $B \times N \times 1 \times 1$, where $B$ denotes the number of mixed samples and $N$ denotes the number of their channels.

$$V_{mean} = \frac{1}{W \times H} \sum_{i=1}^{W} \sum_{j=1}^{H} J(i,j) \tag{8}$$

$$V_{Vx} = \sqrt{\frac{1}{W \times H} \sum_{i=1}^{W} \sum_{j=1}^{H} (I(i,j) - \mu)^2} \tag{9}$$

Where: $I(i,j)$ denotes the mixed sample features; $\mu$ is the mean value; $W$ and $H$ denote the length and width of the mixed sample, respectively.

Then, a convolution unit of size $1 \times 1$ is used to obtain the corresponding enhancement weights from the matrix; finally, a Gaussian distribution is used to reconstruct the enhancement probability distribution from the enhancement weights. The building process is denoted as:

$$P_m \approx N_m\left(h_1(x), t_1^2(x)\right) \tag{10}$$

$$P_v \approx N_v\left(t_2(x), h_2^2(x)\right) \tag{11}$$

Where: $h_1(x)$ and $h_2(x)$ denote the augmented distribution extracted from the mean and variance of the mixed samples, respectively; $t_1(x)$ and $t_2(x)$ are the augmented distributions obtained from the mean and variance of the degenerate samples.

The probability distribution estimation module designed in this paper focuses on the input feature samples at the current stage, so the style migration algorithm (AdaIN) is used to further transform the probability distribution into an overall style migration, i.e., the probability of enhancement distributions of clear images is incorporated into the degraded samples by utilizing the mean, standard deviation, and Gaussian distributions of the mixed samples. This method not only improves the quality of the image, but also improves the generalization ability of the algorithm, and the formula can be expressed as:

$$AdaIN(x) = P_m + \left(\frac{x - h_1(x)}{t_1(x)}\right) \times P_v \tag{12}$$

The testing phase feeds degraded samples directly into the network and improves the image quality by using the probability distribution weights obtained in the training phase.

3.2.3. Loss function. In this paper, the following polynomial loss functions are used to further improve the robustness and generalization of the design network.

1) Enhanced probability distribution loss. To ensure the stability of style migration, this paper uses KL scatter to calculate the extraction parameters of degenerate and mixed samples.

$$V_{KL}\left(P \| Q\right) = \sum P(x) * \log(P(x) / Q(x)) \tag{13}$$

Where: $P$ and $Q$ denote two probability distributions, respectively. The corresponding scatter distributions for the two samples can be expressed:

$$L_1 = V\left(N_m(x) \| \ N_m(y, x)\right) \tag{14}$$

$$L_2 = V\left(N_-(x) \| \ N_-(y, x)\right) \tag{15}$$

Where: $x$ and $y$ denote degraded and mixed sample characteristics, respectively.

2) $L_1$ -loss. In this paper, we mainly use probability distribution combined with style migration to make the network gain enhancement ability, which causes the algorithm to easily lose pixel details, so we use $L_1$ loss function to further enhance the ability to maintain image details. The calculation formula is:

$$L_{L_1} = \frac{1}{W \times H} \sum_{i=0}^{W} \sum_{j=0}^{B} \left| J(i, j) - J'(i, j) \right| \tag{16}$$

Where: $J(i, j)$ and $J'(i, j)$ denote the output image and the corresponding clear image, respectively.

3) Perceptual loss. In order to ensure that the output image further fits the real clear image in the visual senses, the perceptual loss based on VGG-16 is used to calculate the gap between the network output and the clear image with Eq:

$$L_{Poxevplual} = \frac{1}{N}\sum_{i=1}^{x}\left(F_i(J(x)) - F_i\left(J'(x)\right)\right) \tag{17}$$

Where: $F_i(\cdot)$ is the feature representation of the input image in layer $i$ of the VGG-16 network. $N$ denotes the number of total feature layers.

In summary, the total loss function is given by Eq:

$$L = V_{KL} + 0.5L_{L_s} + 0.01L_{Puropplual} \tag{18}$$

### 3.3. Color level enhancement of oil painting based on RGB color balance method

3.3.1. RGB color balance that maintains the mean value of color components. The $R,G,B$ three-channel histogram of a natural clear image is more uniformly distributed and has a higher overlap rate. While the histogram distribution of fuzzy oil paintings is not uniform and the overlap rate is low. Therefore, based on the study of the color distribution of fuzzy oil paintings, this paper proposes a $RGB$ color balance method (RGB-Cbm) that maintains the mean value of the color components, and normalizes each color component with the $R,G,B$ three-channel component mean as the target, so as to make the distribution of the color histogram of fuzzy oil paintings more uniform and the overlap rate is increased, which is close to that of natural and clear images, so as to achieve the purpose of color balance and color correction.

The specific process of Gray World Algorithm (GWA) is as follows: firstly, calculate the mean value of each color channel of the input image, then get the high pixel value and low pixel value of each color channel by calculating the quartile, and finally bring the equation (1) to get the processed image.

$$I^c = F\left\{\left[m\left(I^s\right) + m\left(I^g\right) + m\left(I^b\right)\right] \div 3 + \frac{I^c - m\left(I^c\right)}{h\left(I^c\right) - l\left(I^c\right)}\right\} \tag{19}$$

Where: $I^c$ is the color channel of the input image; $m\left(I^c\right)$ is the mean value of the computed color channel; $h\left(I^c\right)$ and $l\left(I^c\right)$ are the high and low pixel values of the computed color channel, $F$ is the bilateral filtering to remove the noise and $c$ is taken as $r,g,b$.

3.3.2. Multiscale Retinex Enhancement Algorithm with Color Recovery. The Retinex algorithm has a long history as a very widely used image enhancement method. It is also known as the color constancy theory, which means that the color of an object is not affected by the non-uniformity of light and has consistency. After years of improvement, Retinex algorithm has reached a balance between edge enhancement, color constancy and dynamic range compression, and it is still a popular image enhancement method because it can adaptively enhance different types of images.

Currently, Retinex algorithms mainly include single-scale Retinex (sSR), multi-scale Retinex (MSR), and multi-scale Retinex with color recovery (MSRCR). In this paper, MSRCR is chosen as a part of image enhancement because MSRCR can recover some details while further enhancing the color of the image. The specific implementation is as follows:

$$MSRCR(x,y)' = g \cdot MSRCR(x,y) + b \tag{20}$$

$$MSRCR(x,y) = C(x,y)MSR(x,y) \tag{21}$$

$$C(x,y) = \beta\left\{\log\left[\alpha \cdot I^c(x,y)\right] - \log\left[\sum_{c=1}^{3} I^c(x,y)\right]\right\} \tag{22}$$

$$MSR(x,y) = \sum_{i=1}^{n} w_i\left\{\log I^c(x,y) - \log\left[I^c(x,y)\cdot G_i(x,y)\right]\right\} \tag{23}$$

Where: $g$ is the gain, $b$ is the deviation. $C$ is the color recovery factor for each color channel, which regulates the scale of the color channels. $\beta$ is the gain constant, $\alpha$ is the controlled nonlinear intensity, $I^c(x,y)$ is the image of a particular channel; $n$ is the number of scales, $w_i$ is the weights; $G_i$ is the Gaussian filtering.

3.3.3. Relative global histogram stretching. The traditional global histogram stretching is to use the same parameters for all the channels of the image, which will ignore the characteristics of the different distributions of different channels, resulting in overstretching or understretching, reducing the effect of image enhancement and causing loss of details. In this paper, the relative global histogram stretching (RGHS) is used according to the color distribution law of fuzzy oil paintings, and this algorithm can effectively improve the contrast correction effect of degraded images, and the adaptive parameter design avoids the overstretching or understretching of the histogram. RGB-Cbm is used in the actual application process, which omits the step of image preprocessing by GWA in the original text. The algorithm is formulated as follows:

$$P' = \left(P - I_{\min}\right)\left(\frac{O_{\max} - O_{\min}}{I_{\max} - I_{\min}}\right) + O_{\min} \tag{24}$$

Where: $P'$ and $P$ are the output and input pixels, respectively; $I_{\min}$, $I_{\max}$, $O_{\min}$, $O_{\max}$ are the adaptive parameters of the image before and after histogram stretching, respectively. The specific acquisition process is as follows:

1) Acquisition of $I_{\min}$, $I_{\max}$. The peak mode $v$ of the image histogram is similar to the midpoint of the histogram, so the midpoint is used as the dividing line to determine the maximum and minimum values of the input image adaptive parameters during the histogram stretching process. Since extreme pixel values can easily exist in fuzzy oil paintings, the range of histogram stretching is set from 0.1% to 99.9%. The specific formula is as follows:

$$I_{\min} = P_s\left[P_s.\ index\ (v) \times 0.1\%\right] \tag{25}$$

$$I_{\max} = P_s\left[-\left(P.len - P.index(v)\right) \times 0.1\%\right] \tag{26}$$

Where: $P$ is the set of image pixels for each channel; $P_s$ is the set after sorting $P$ in ascending order; $P_s.index(v)$ is the index number of the peak mode $v$ in the histogram distribution. The smallest 0.1% of the total number of pixels on the left side of the peak mode and the largest 0.1% of the total number of pixels on the right side are removed from the histogram to reduce the effect of extreme pixel values on the histogram stretching.

2) Acquisition of $O_{\min}$, $O_{\max}$. In order to reduce the negative effect of uneven color distribution of degraded images on image color recovery, the parameter $k_c$ is used to represent the gap between each channel of degraded image and the clear natural image, and the specific formula is as follows:

$$k_c = 0.5 / m\left(I^c\right) \tag{27}$$

$$O_{\max} = I^c / k_c t_c \tag{28}$$

$$t_c = m\left[t_c(x)\right] \tag{29}$$

where $t_c(x)$ is the refractive index of each channel.

The histogram distribution of the $R$, $G$, and $B$ color channels of the degraded mass image is similar to the Rayleigh distribution, i.e:

$$RD_c = \frac{x}{v_c^2} e^{\frac{-x^2}{v_c^2}} \tag{30}$$

Where: $x$ is the pixel point, $c \in \{R, G, B\}$, $v$ are the scale parameters of the distribution i.e. the peak mode of the image histogram. From this the variance $\sigma$ of the distribution can be obtained and the $O_{\min}$ parameter is derived:

$$\sigma = \sqrt{(4-\pi)/2} \cdot v \tag{31}$$

$$O_{\min} = v_c - \sigma_c \tag{32}$$

3.3.4. Adaptive stretching of Lab color space. After the above processing, an adaptive stretching of the Lab color space (LabS) is performed to improve the color and luminance correction of the image.In Lab color space, the $L$ component represents the luminance, with 100 being the brightest and 0 being the darkest, and the $a$ and $b$ components are used to control the color balance, with a range of $[-128, 127]$, and when both are 0, the image appears gray.

Specifically, this includes adjusting the overall brightness of the image using the $L$ component, stretching $[0.1\% \sim 99.9\%]$ t o $[0 \sim 100]$, and setting the values below 0.1% as well as above 99.9% to 0 and 100, respectively; and then making modifications to the $a$, $b$ component, and then stretching, which allows for accurate color correction.

$$I_c' = I_c \times \varphi^{1-\left|\frac{I_r}{128}\right|} \tag{33}$$

Where: $I_c'$ and $I_c$ are the output and input pixels; according to the experiment, $\varphi$ is set to 1.5. After stretching, the image is reconverted to RGB color space to get the final output image.

## 4. Simulation analysis of image enhancement algorithms

Since there is no publicly available large-scale fuzzy oil painting dataset, we use a web crawler to collect about 4000 images with the keyword "oil painting" on the Internet, and then manually screen out 1100 images of real scenes and a small dataset of 200 fuzzy oil paintings with fuzzy oil paintings collected by the authors themselves, totaling about The total number of fuzzy oil paintings is about 1500 for the simulation experiment.

### *4.1. Analysis of image color deviation correction effect*

The image histogram visualizes the frequency of occurrence of each gray level in an image and describes the statistical characteristics of the image color. Literature suggests that in RGB space, the histograms of oil painting images are sequential, shifted and concentrated, i.e., the three-channel histograms of normal images have a large overlap, while the histograms of blurred oil paintings are sequentially shifted in the order of blue, green, and red and have a small pixel-value distribution interval, and the histograms are characterized by a sharp peak shape. In the opposing color space, opposing color channels are used to describe various colors, and the strongly attenuated blue light and enhanced yellow light information in the blurred oil painting will lead to its opposing color information being too large or too small. Figures 2 and 3 show the histogram distributions of blurred oil paintings under different degrees of blurring in the two color spaces for the less blurred and more blurred cases, respectively; Figures 2(a)~(c) show the RGB, Lab, and YUV histograms for the less blurred case, and Figures 3(a)~(c) show the RGB, Lab, and YUV histograms for the more blurred case.

In Lab space, the L component represents the luminance; the a and b components are two opposing color channels, which represent the change from green to red and the change from blue to yellow, respectively. Due to the strong attenuation of blue information and over-enhancement of yellow information in the blurred oil painting, there will be a slightly larger a-channel pixel value and a larger b-channel pixel value, which is shown in the histogram as the a-channel is slightly shifted to the right and the b-channel is shifted to the right. In YUV space, the Y component represents luminance, the U component represents blue chromaticity information through the difference between green and blue, and the V component represents red chromaticity information through the difference between red and blue. For blurred canvases, there will be a small biased U component and a large biased V component, which is shown in the histogram as a left shift of the U channel and a right shift of the V channel.

Observation and analysis of all the histograms of fuzzy oil paintings in the test set constructed in this paper shows that the histograms of fuzzy oil paintings in Lab and YUV space also show the order and offset in RGB space, i.e., the two color channels are shifted in the order of a and b from left to right in Lab space, and the two color channels are shifted in the order of U and V from left to right in YUV space, and the more fuzzy the clarity of the image is, the larger the offset of the two color channels is. And the blurrier the image clarity, the larger the offset of the two color channels. According to the offset law of the histogram of the fuzzy oil painting, the histogram can be corrected to eliminate the color deviation, or to judge whether the image still has color deviation according to the distribution of the histogram.

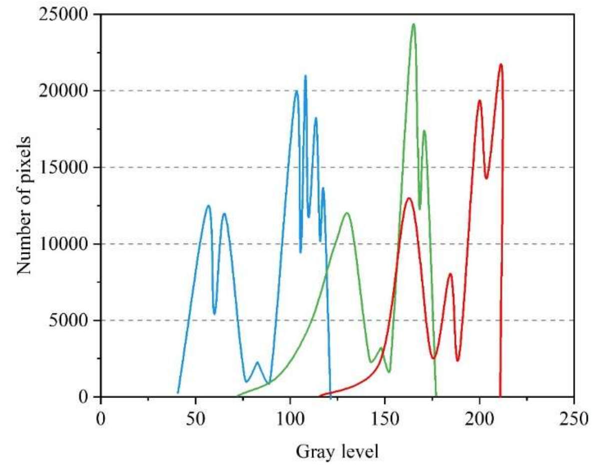


(a)The RGB histogram of the blur is lighter

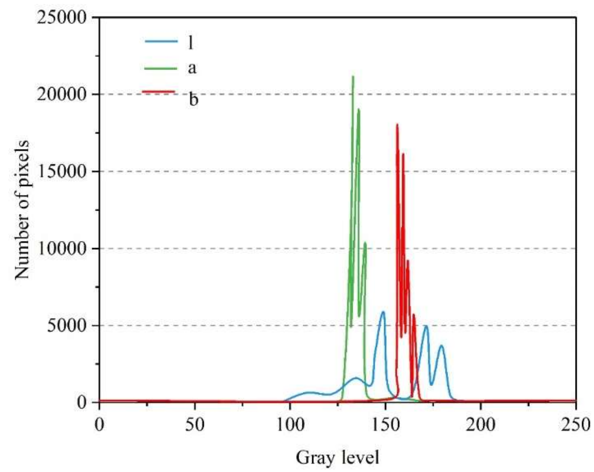


(b)Lab histogram under the blur is lighter

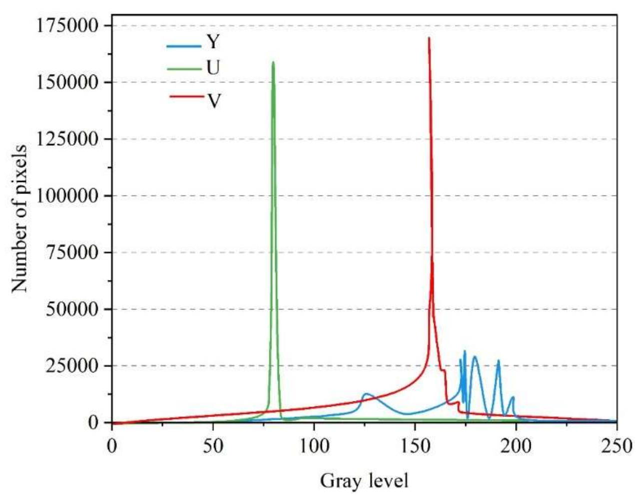


(c)The YUV histogram of the blur is lighter

**Fig. 2.** The blur is lighter

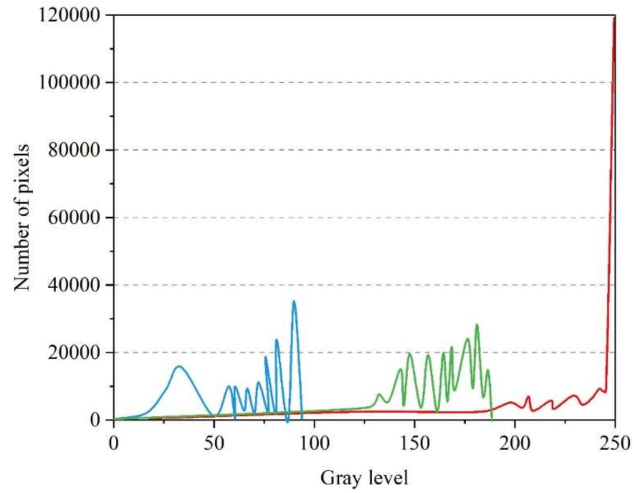


(a)RGB histogram in fuzzy degree

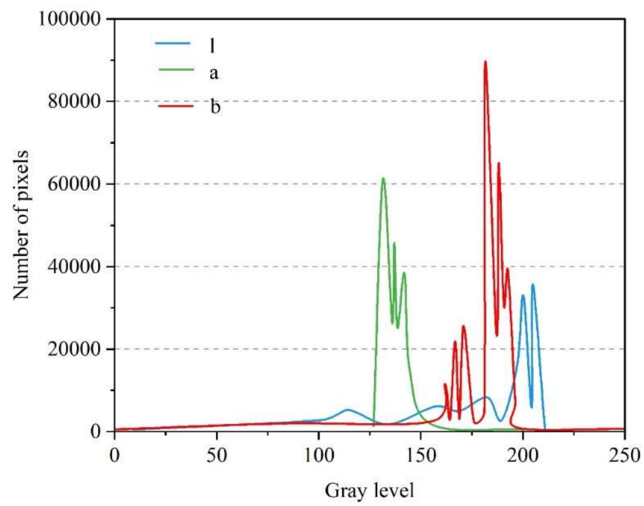


(b)Lab histogram under fuzzy degree

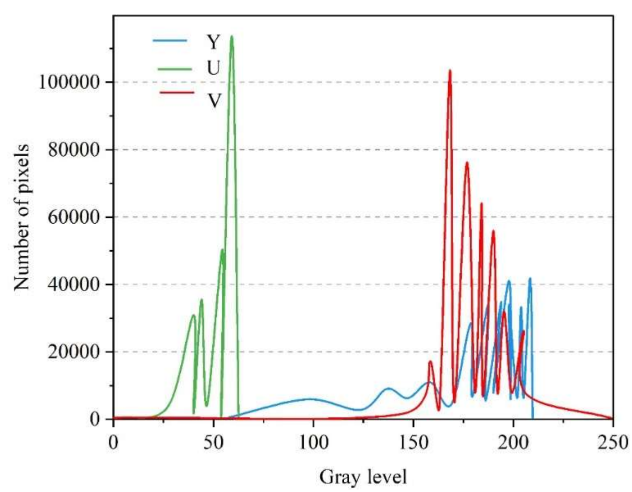


(c)YUV histogram under fuzzy degree

**Fig. 3.** Fuzzy degree

The results of the bias correction are shown in Fig. 4-Fig. 6. Fig. 4, Fig. 5, and Fig. 6 show the histogram of the blurred oil painting, the image without luminance stretching, and the image after luminance stretching, respectively. Figure 4 shows its corresponding Lab space histogram, which shows that the a and b channels are sequentially shifted. Figure 5 shows the histogram of the image without luminance stretching, and it is seen that the offsets of the a and b channels have been corrected, but the luminance channel distribution interval is small. Figure 6 shows the corresponding histogram of the image after luminance stretching, the luminance channel distribution is more uniform and the overall interval is improved.

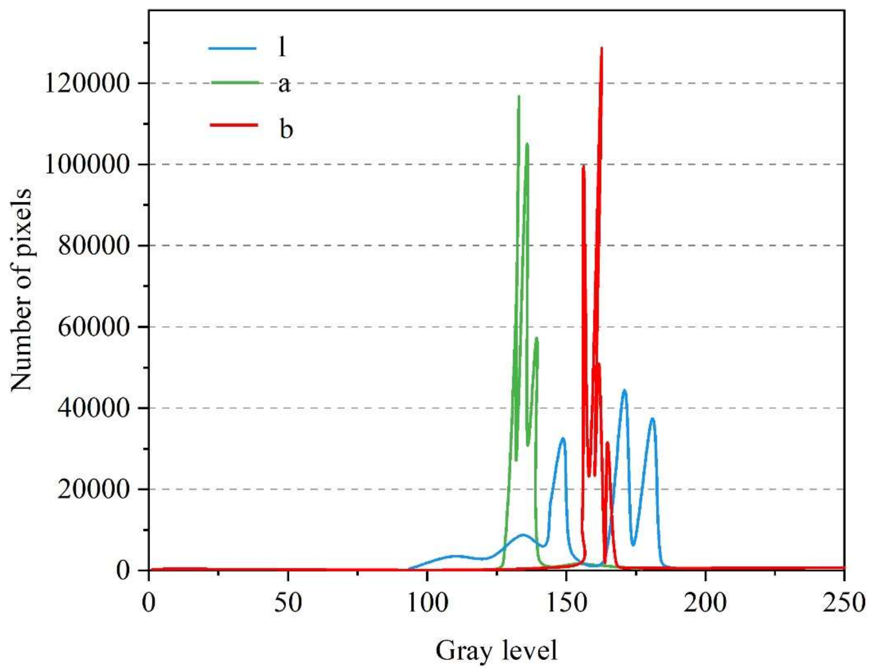


**Fig. 4.** Histogram of image

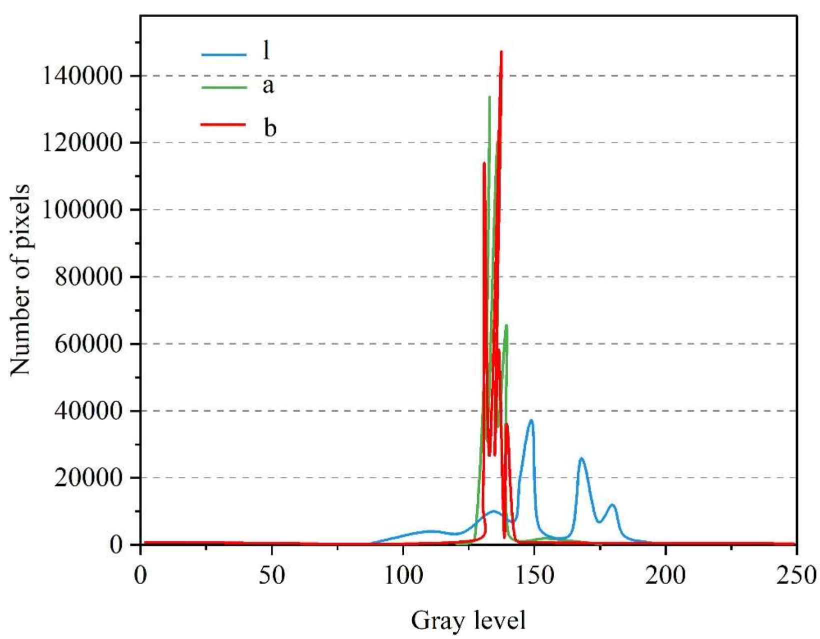


**Fig. 5.** No image of brightness stretching

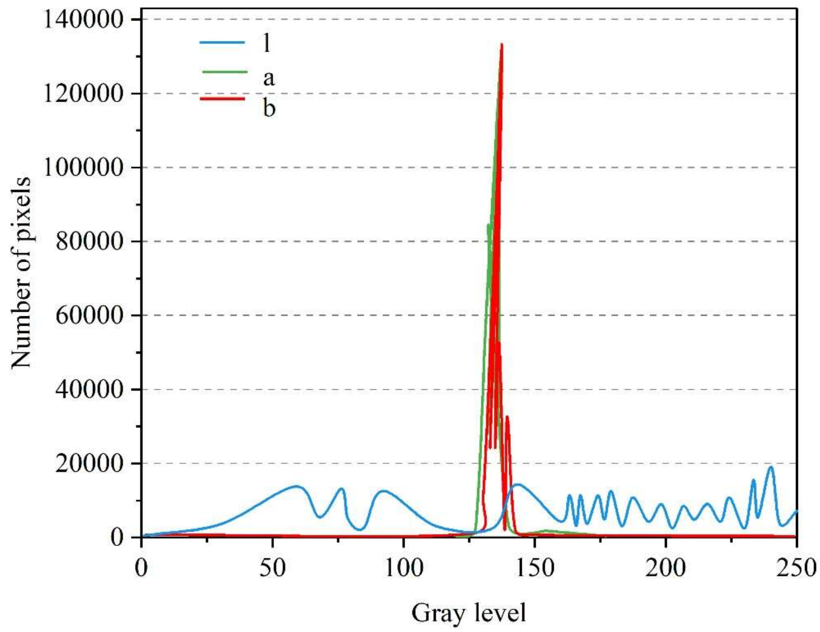


**Fig. 6.** The image of the brightness stretching

In order to verify the feasibility of the algorithms in this paper, five advanced fuzzy oil painting enhancement algorithms are selected as comparison algorithms for the experiments, the comparison algorithms are: fusion-based enhancement (FBE) algorithm, normalized gamma transform (NGT) algorithm, successive color balancing (SCB) algorithm, Fourier transform (FT) algorithm, halo subtracted dark channel prior (HRDCP) algorithm. The images used for the experiments are from the image dataset constructed in this paper. The experimental environment was selected as Windows 10 system, CPU intel CORE i7-7700HQ, RAM 8 GB. The programming languages are Python and MATLAB.

At present, there is no unified evaluation standard and dedicated quantitative index for fuzzy oil painting, therefore, four more commonly used reference-free image quality evaluation indexes are selected to objectively analyze the enhancement effect of the algorithm: natural image quality evaluation (NIQE), image quality evaluation based on reference-free perception (PIQE), based on the reference-free image spatial domain quality evaluation (BRISQUE), and entropy-based reference-free image quality evaluation (ENIQA). Reference Image Quality Assessment (ENIQA).The smaller the score of the four evaluation indexes, the better the image quality. Table 1 shows the average values of each index after each algorithm processes 50 experimental images with different degrees of contamination. Among them, NGT achieved the best NIQE performance, this paper's algorithm scored the second place, and the FBE algorithm also achieved a good score. For PIQE, this paper's algorithm is optimal and stronger than the NGT algorithm, which improves by 3.129 compared to NGT.For BRISQUE, this paper's algorithm is basically equal to SCB, maintaining a slight advantage, and the NGT algorithm also has a better performance. For ENIQA, this paper's algorithm outperforms the other five algorithms, and the NGT algorithm is slightly weaker than this paper's algorithm. Combining the four evaluation metrics, the FBE algorithm has better NIQE metrics, and the rest of the metrics have average performance. The HRDCP algorithm performs comparable to its subjective effect in quantitative metrics and is weaker than the other algorithms.The NGT algorithm performs better in quantitative metrics.The SCB algorithm and the FT algorithm also achieve better results. The algorithms in this paper have the best overall performance, except for NIQE which is weaker than NGT algorithm.

**Table 1.** Comparison of quantitative metrics of algorithms

| Evaluation index | FBE | HRDCP | NGT | SCB | FT | This algorithm |
|---|---|---|---|---|---|---|

| | | | | | | |
|---|---|---|---|---|---|---|
| NIQE | 3.089 | 4.149 | 2.77 | 3.271 | 3.476 | 2.993 |
| PIQE | 39.201 | 39.664 | 35.961 | 37.042 | 40.199 | 32.832 |
| BRISQUE | 31.294 | 28.242 | 22.558 | 20.067 | 26.76 | 20.065 |
| ENIQA | 0.241 | 0.169 | 0.123 | 0.142 | 0.163 | 0.113 |

### *4.2. Analysis of the effect of image picture hierarchy enhancement*

In order to better verify the effectiveness of the method proposed in this paper, the experimental results of the image quality enhancement experiments on five oil paintings numbered A, B, C, D and E by six different methods, namely, this paper's algorithm, Fourier Transform (FT), Wavelet Transform (WT), High-Frequency Enhancement Filtering (HFEF), Low-Frequency Enhancement Filtering (LPF), and SCB, are evaluated in the paper using the more classical objective evaluation indexes. . The objective evaluation metrics include: feature similarity FSIM, mean square error NMSE, structural similarity SSIM, peak signal-to-noise ratio PSNR, and image enhancement factor IEF.It is important to note that for FSIM, SSIM, PSNR, and IEF, the larger the evaluated value represents the better quality of the image, whereas for the NMSE metrics, the smaller the evaluated value indicates a better quality of the image. The evaluation results of different indicators are shown in Table 2, the results obtained by the algorithm in this paper are higher than the traditional methods in terms of the classical objective evaluation indicators, and the FSIM of this paper's algorithm is 0.9999, which is very close to 1. This indicates that the resultant images obtained by the algorithm in this paper have a better performance in terms of objective evaluation.

**Table 2.** Objective score results

| Group number | Method | FSIM | NMSE | SSIM | PSNR | IEF |
|---|---|---|---|---|---|---|
| A | FT | 0.993 | 0.2273 | 0.7883 | 55.0993 | 0.0372 |
| | WT | 0.989 | 0.1637 | 0.7845 | 56.5296 | 0.0367 |
| | HFEF | 0.9835 | 0.1103 | 0.6761 | 58.239 | 0.0421 |
| | LPF | 0.9900 | 0.1849 | 0.7681 | 55.9897 | 0.0463 |
| | SCB | 0.9798 | 0.3996 | 0.7 | 55.1764 | 0.0479 |
| | This method | 0.9988 | 0.0432 | 0.7893 | 62.3187 | 0.0546 |
| B | FT | 0.994 | 0.1829 | 0.3333 | 57.2262 | 0.0199 |
| | WT | 0.9951 | 0.0989 | 0.1547 | 57.9437 | 0.0327 |
| | HFEF | 0.9997 | 0.0546 | 0.766 | 62.7655 | 0.0479 |
| | LPF | 0.9832 | 0.4871 | 0.2691 | 58.8446 | 0.0172 |
| | SCB | 0.9925 | 0.3681 | 0.363 | 56.983 | 0.0331 |
| | This method | 0.9996 | 0.0175 | 0.7681 | 67.5576 | 0.0338 |
| C | FT | 0.994 | 0.3966 | 0.2455 | 55.7149 | 0.0253 |
| | WT | 0.9979 | 0.2144 | 0.3197 | 57.6653 | 0.0289 |
| | HFEF | 0.9984 | 0.0456 | 0.2625 | 61.705 | 0.0245 |
| | LPF | 0.9882 | 0.1147 | 0.3278 | 59.542 | 0.0226 |
| | SCB | 0.9889 | 0.8288 | 0.1969 | 54.2077 | 0.0298 |
| | This method | 0.9998 | 0.0383 | 0.3711 | 62.4521 | 0.0322 |
| D | FT | 0.9947 | 0.2154 | 0.2394 | 54.7265 | 0.0339 |
| | WT | 0.9907 | 0.4852 | 0.2891 | 57.2233 | 0.0306 |
| | HFEF | 0.9989 | 0.0558 | 0.6736 | 60.5826 | 0.0329 |

| | | | | | | |
|---|---|---|---|---|---|---|
| | LPF | 0.997 | 0.1166 | 0.7031 | 57.3953 | 0.0209 |
| | SCB | 0.9891 | 0.5889 | 0.1787 | 53.7006 | 0.035 |
| | This method | 0.9999 | 0.0186 | 0.7946 | 65.2799 | 0.0392 |
| E | FT | 0.9793 | 0.3083 | 0.2048 | 56.9257 | 0.0342 |
| | WT | 0.9742 | 0.1832 | 0.1748 | 59.1967 | 0.0317 |
| | HFEF | 0.9829 | 0.3881 | 0.2258 | 55.9254 | 0.0331 |
| | LPF | 0.9638 | 0.2265 | 0.1709 | 58.2569 | 0.0334 |
| | SCB | 0.9863 | 0.3177 | 0.2134 | 57.313 | 0.0292 |
| | This method | 0.9982 | 0.1102 | 0.2845 | 61.4019 | 0.0342 |

In order to assess the effectiveness of the proposed algorithm of this paper more comprehensively, the paper specially traveled to venues full of artistry and randomly invited 50 volunteers (20 boys and 20 girls) with certain aesthetic literacy in oil painting to make subjective evaluations of the experimental results shown in oil paintings A-E, which were comprehensively scored on a 10-point scale from three aspects, namely, hierarchy retention, detail retention, and visual effect, respectively. In this case, the score of each method was the mean value of the ratings of 4050 volunteers, and the higher mean value of the ratings indicated the better quality of the image. The final scoring results are shown in Table 3. The subjective scores of this paper's algorithms are all higher than other methods in the paper, and the average subjective score of the three aesthetic dimensions of this paper's methods is 9.15, which further confirms the effectiveness of the new methods in the paper.

**Table 3.** Subjective evaluation results

| Method | FT | WT | HFEF | LPF | SCB | This method |
|---|---|---|---|---|---|---|
| Hierarchical feeling | 8.03 | 8.44 | 8.76 | 7.93 | 8.64 | 9.05 |
| Detail retention | 8.65 | 8.24 | 8.62 | 8.03 | 8.33 | 9.08 |
| Visual effect | 8.03 | 8.32 | 8.75 | 8.47 | 8.61 | 9.31 |

### 4.3. *Example application effect analysis*

This study takes oil painting portrait series as an example. The oil painting portrait series has collected seven different portrait drawings, using different colors to distinguish the appearance elements of the portrait, which is convenient for the measurement and calculation of the beauty index in the later stage, of which samples 4 and 7 come from the portrait oil painting samples after the algorithm of this paper has been processed for the enhancement of picture hierarchy, and the rest of the samples are unprocessed.

Balance (balance, form center offset), proportion (proportionality), rhythm (order), coordination (wholeness, density, similarity proportion) and unity (common direction, simplification) are selected as the beauty factors to construct the quantitative system. According to the nine selected beauty indicators, the coordinate system of portrait appearance parameter measurement is drawn. The origin O of the coordinate system is the center of the portrait, and the cross point o is the center of each cosmetic element. Use the appearance analysis software to map the relevant beauty factor data, and calculate the value of each beauty index. Take the balance degree calculation of sample 1 as an example. Sample 1 contains three elements, numbered from left to right as Element 1, Element 2, Element 3. beauty index measurement data obtained by software measurement. Substitute the measured data in Table 4 into the balance index calculation formula to get the vertical balance of sample 1 as, horizontal balance and balance. Calculate the rest of the beauty index of sample 1. Calculate the beauty index of other samples with reference to sample 1. The simplification degree of the 7 portrait samples is calculated to be 0.339, so the simplification degree is no longer considered in the quantitative system of beauty indicators. Calculate the remaining 8 indicators to get the morphological beauty index matrix X. The morphological beauty index matrix is shown in Table 4.The morphological beauty index matrix X is standardized according to the formula. The standardized matrix is shown in Table 5. The sample weight value of each beauty indicator is calculated and the sample weight value is shown in Table 6. The entropy value and weight of each beauty index is shown in Table 7, and Dph Dpy Dbl Dcx Dxs Dzt Dmj Dfx represents the degree of balance, the degree of form-centered offset, the degree of proportionality, the degree of order, the degree of wholeness, the degree of denseness, the degree of similarity proportionality, and the degree of common direction, respectively.

Calculate the relative entropy of the samples. The matrix of beauty indicators is vertically standardized to obtain the weight value of the beauty indicators of each sample, and the weight value of the beauty indicators of each sample is shown in Table 8. After obtaining the entropy value of each sample, when the specific gravity of each beauty indicator is completely equal, the entropy takes the maximum value of Simax=ln(8), and the relative entropy of each sample is calculated. The standardized matrix, the weight matrix W of the beauty indicators and the relative entropy data of each sample are calculated comprehensively to get the comprehensive evaluation results of the beauty of oil painting portrait series, and the relative entropy value and the comprehensive evaluation results of the beauty are shown in Table 9.

From the comprehensive evaluation results, it can be seen that the rating of sample 7 is the highest, and the rating of sample 4 is the second highest, therefore, these two portrait oil paintings are selected as representative samples to be analyzed to verify the reasonableness of the results of the evaluation of the degree of beauty.

The layout of Sample 4's character facial features adopts left-right symmetry, with soft facial edges, clear painting lines, and a strong sense of hierarchy in the picture. The morphological features of the characters in Sample 7 are generally consistent with those in Sample 4, with soft facial edges and less angularity. And the skin texture is delicate. From the perspective of comprehensive evaluation of beauty indexes, the two high-weight indexes (proportionality, common direction) have higher ratings, thanks to their more popular morphological features of character appearance and the consideration of the proportion of character appearance elements, which are close to the classical proportion of portrait oil painting, indicating that the effect of the image enhancement technology in this paper is in line with the popular aesthetics of oil paintings.

In summary, the analysis results of the portrait oil paintings of Sample 4 and Sample 7 have high beauty ratings in line with the aesthetic requirements of the art of oil painting and the mainstream trend of beauty, which verifies the reasonableness and acceptance of the comprehensive evaluation method of beauty for the quantification of the beauty of the figure form layout, and at the same time verifies that the image hierarchy enhancement technology of this paper's oil paintings provides an intelligent optimization direction for painters to carry out portrait paintings.

**Table 4.** Matrix of form aesthetic measure

| | Sample1 | Sample2 | Sample3 | Sample4 | Sample5 | Sample6 | Sample7 |
|---|---|---|---|---|---|---|---|
| Balance | 0.133 | 0.064 | 0.552 | 0.514 | 0.453 | 0.513 | 0.405 |
| Profile shift | 0.925 | 0.847 | 0.968 | 0.986 | 0.862 | 0.871 | 0.819 |
| Proportionality | 0.842 | 0.827 | 0.757 | 0.671 | 0.569 | 0.544 | 0.671 |
| Sense of order | 1.000 | 0.753 | 0.497 | 1.000 | 0.996 | 0.995 | 1.000 |
| Similarity ratio | 0.662 | 0.687 | 0.801 | 0.71 | 0.74 | 0.604 | 0.845 |
| Overall degree | 0.431 | 0.624 | 0.341 | 0.851 | 0.273 | 0.629 | 0.813 |
| Intensity | 0.909 | 0.867 | 0.921 | 0.923 | 0.956 | 0.934 | 0.847 |

| | | | | | | | |
|---|---|---|---|---|---|---|---|
| Common direction | 0 | 0 | 0.336 | 0.334 | 0.335 | 0.166 | 0.401 |

**Table 5.** Normalized matrix

| | Sample1 | Sample2 | Sample3 | Sample4 | Sample5 | Sample6 | Sample7 |
|---|---|---|---|---|---|---|---|
| Balance | 0.139 | 0.001 | 0.998 | 0.92 | 0.792 | 0.93 | 0.709 |
| Profile shift | 0.366 | 0.802 | 0.110 | 0.002 | 0.688 | 0.675 | 1.000 |
| Proportionality | 0.003 | 0.044 | 0.284 | 0.552 | 0.908 | 0.995 | 0.567 |
| Sense of order | 1.000 | 0.501 | 0.003 | 0.999 | 1.000 | 1.000 | 1.004 |
| Similarity ratio | 0.249 | 0.37 | 0.835 | 0.435 | 0.58 | 0.002 | 1.000 |
| Overall degree | 0.273 | 0.604 | 0.113 | 1.000 | 0.001 | 0.611 | 0.927 |
| Intensity | 0.416 | 0.848 | 0.334 | 0.306 | -0.002 | 0.225 | 0.999 |
| Common direction | 0.001 | 0.001 | 0.833 | 0.835 | 0.837 | 0.415 | 0.997 |

**Table 6.** Sample proportion values

| | Sample1 | Sample2 | Sample3 | Sample4 | Sample5 | Sample6 | Sample7 |
|---|---|---|---|---|---|---|---|
| Balance | 0.037 | 0.002 | 0.225 | 0.206 | 0.18 | 0.2 | 0.150 |
| Profile shift | 0.105 | 0.217 | 0.024 | 0.001 | 0.194 | 0.187 | 0.272 |
| Proportionality | 0.001 | 0.015 | 0.086 | 0.165 | 0.268 | 0.301 | 0.164 |
| Sense of order | 0.174 | 0.093 | 0.002 | 0.178 | 0.184 | 0.182 | 0.187 |
| Similarity ratio | 0.076 | 0.108 | 0.245 | 0.123 | 0.169 | 0.004 | 0.275 |
| Overall degree | 0.079 | 0.168 | 0.028 | 0.281 | 0.001 | 0.172 | 0.271 |
| Intensity | 0.137 | 0.272 | 0.107 | 0.096 | 0.001 | 0.071 | 0.316 |
| Common direction | 0.0010 | 0.002 | 0.216 | 0.216 | 0.215 | 0.102 | 0.248 |

**Table 7.** Entropy values & weights

| | Dph | Dpy | Dbl | Dcx | Dxs | Dzt | Dmj | Dfx |
|---|---|---|---|---|---|---|---|---|
| Entropy | 0.876 | 0.852 | 0.816 | 0.907 | 0.868 | 0.839 | 0.847 | 0.815 |
| Weighting | 0.112 | 0.125 | 0.159 | 0.076 | 0.105 | 0.139 | 0.130 | 0.154 |

**Table 8.** Proportions of aesthetic measures

| | Sample1 | Sample2 | Sample3 | Sample4 | Sample5 | Sample6 | Sample7 |
|---|---|---|---|---|---|---|---|
| Balance | 0.028 | 0.019 | 0.103 | 0.083 | 0.089 | 0.094 | 0.074 |
| Profile shift | 0.192 | 0.181 | 0.19 | 0.174 | 0.165 | 0.161 | 0.141 |
| Proportionality | 0.167 | 0.177 | 0.152 | 0.118 | 0.11 | 0.11 | 0.124 |
| Sense of order | 0.21 | 0.158 | 0.101 | 0.169 | 0.197 | 0.191 | 0.173 |
| Similarity ratio | 0.133 | 0.147 | 0.16 | 0.118 | 0.143 | 0.119 | 0.145 |
| Overall degree | 0.085 | 0.135 | 0.064 | 0.143 | 0.05 | 0.121 | 0.138 |
| Intensity | 0.189 | 0.182 | 0.174 | 0.154 | 0.185 | 0.177 | 0.143 |
| Common direction | -0.004 | 0.001 | 0.063 | 0.057 | 0.07 | 0.037 | 0.072 |

**Table 9.** Relative entropy values & integrated evaluations of aesthetic

| | Dph | Dpy | Dbl | Dcx | Dxs | Dzt | Dmj | Dfx |
|---|---|---|---|---|---|---|---|---|
| Relative entropy | 1.847 | 1.846 | 2.011 | 2.031 | 1.992 | 1.996 | 2.036 | 1.847 |
| Comprehensive evaluation | 0.232 | 0.333 | 0.436 | 0.603 | 0.561 | 0.568 | 0.872 | 0.232 |

## 5. Conclusion

In this paper, we propose a texture enhancement network based on positive probability distribution guidance and an RGB color balancing method that maintains the mean value of color components for the picture level enhancement problem in oil paintings.

Firstly, the offset laws of the histograms of oil painting images in Lab and YUV color spaces are summarized, and the bias correction and luminance stretching of oil painting images are carried out in Lab space, and then the existing state-of-the-art algorithms are compared and analyzed with the algorithm of this paper. The four quantization indexes are chosen again, except NIQE is only weaker than NGT algorithm, the other three indexes of this paper's algorithm are improved, and PIQE is improved by 3.129 compared with NGT. The comprehensive performance is ahead of the rest of the algorithms, and this paper's algorithm has the best overall performance.

Compared with the traditional methods, the proposed method in this paper achieves better performance in three subjective evaluation levels of hierarchy, detail and visual effect, and several objective evaluation indexes, such as PNSR, SSIM, NMSE, IEF, FSIM, and so on. The FSIM of this paper's algorithm reaches 0.9999 during the image enhancement experiment on the oil painting numbered D. This illustrates the effectiveness of this paper's algorithm.

This study quantitatively analyzes the beauty index of oil paintings. Taking the oil painting portrait series as an example, through the analysis of the similarity of the morphological layout of sample 4 and sample 7 with high comprehensive score of beauty, it verifies the effectiveness of the method of this paper, which improves the efficiency of the painter's painting to a certain extent.

## Funding

This work was supported by Anhui Province Philosophy and Social Sciences Planning Project: “Regional Characteristics of ‘New Anhui School Oil Painting’ and Its Aesthetic Research” (AHSKY2020D112).

## References

[1] Van der Veen, M. (2021). Crossroads of seeing: about layers in painting and superimposition in Augmented Reality. AI & SOCIETY, 36(4), 1189-1200.

[2] Brey, J. A., & Waller, J. (2016). Layers: an art and Earth science collaborative exhibition of paintings and text. Bulletin of the American Meteorological Society, 97(2), 278-284.

[3] Cohen, J. (2016). Chromatic layering and color relationalism. Minds and Machines, 26, 287-301.

[4] Su, Z. B., Su, Y. N., Suo, Y. H., & Ren, H. (2019, June). Effect of Colored Content on Depth Perception of S3D Images. In 2019 IEEE/ACIS 18th International Conference on Computer and Information Science (ICIS) (pp. 140-144). IEEE.

[5] Gilson, E. (2023). Painting and reality. Princeton University Press.

[6] Thomopoulos, N. T., Thomopoulos, N. T., & Philipson. (2018). Probability Distributions. Springer.

[7] Lebedev, A. V. (2019). The nontransitivity problem for three continuous random variables. Automation and Remote Control, 80, 1058-1068.

[8] Mitov, K. V., & Nadarajah, S. (2022). Limit distributions for the maxima of discrete random variables under monotone normalization. Lithuanian Mathematical Journal, 1-11.

[9] Khalid, S., Azad, M. M., Kim, H. S., Yoon, Y., Lee, H., Choi, K. S., & Yang, Y. (2024). A Review on Traditional and Artificial Intelligence-Based Preservation Techniques for Oil Painting Artworks. Gels, 10(8), 517.

[10] Taha, E., Mohie, M. A., Korany, M. S., Aly, N., Ropy, A., & Negem, M. (2024). Coatings containing molybdenum trisulphide QDs to protect oil paintings against different environmental factors. Pigment & Resin Technology, 53(4), 450-458.

[11] Kim, J., Jun, J. Y., Hong, M., Shim, H., & Ahn, J. (2019). Classification of oil painting using machine learning with visualized depth information. The International Archives of the Photogrammetry, Remote Sensing and Spatial Information Sciences, 42, 617-623.

[12] Liu, Y. (2021). Improved generative adversarial network and its application in image oil painting style transfer. Image and Vision Computing, 105, 104087.

[13] Liu, X. (2022). An Improved Oil Painting Formation Using Advanced Image Processing. Mobile Information Systems, 2022(1), 4865060.

[14] Shree Prakash & Jagadeesh Kakarla. (2023). Three level automatic segmentation of optic disc using LAB color space contours and morphological operation. International Journal of Imaging Systems and Technology(5),1796-1813.

[15] Fengqi Guo,Jingping Zhu,Liqing Huang,Feng Li,Ning Zhang,Jinxin Deng... & Xun Hou. (2024). Multi-Dimensional Fusion of Spectral and Polarimetric Images Followed by Pseudo-Color Algorithm Integration and Mapping in HSI Space. Remote Sensing(7),

[16] Shengjie Wang,Deng Pan,Xianda Chen,Zexin Duan & Zehao Xu. (2025). Connected vehicle following control based on gated recurrent unit with attention mechanism. Engineering Applications of Artificial Intelligence109820-109820.